Journal of ELECTRONIC MATERIALS, Vol. 46, No. 2, 2017
DOI: 10.1007/s11664-016-4982-7

Thermal and Electrical Conductivity of $Ge_1Sb_4Te_7$ Chalcogenide Alloy

RUI LAN,[1,4] RIE ENDO,[2] MASASHI KUWAHARA,[3] YOSHINAO KOBAYASHI,[2] and MASAHIRO SUSA[2]

1.—School of Material Science and Technology, Jiangsu University of Science and Technology, No. 2, Mengxi Road, Zhenjiang City 212003, Jiangsu Province, China. 2.—Department of Metallurgy and Ceramics Science, Tokyo Institute of Technology, Ookayama, Meguro-Ku, Tokyo 152-8552, Japan. 3.—Photonics Research Institute, National Institutes of Advanced Industrial Science and Technology, 1-1-1 Higashi, Tsukuba-shi, Ibaraki 305-8562, Japan. 4.—e-mail: dutrlan@just.edu.cn

The unique properties of the $Ge_1Sb_4Te_7$ alloy as a chalcogenide make it a good candidate for application in phase-change random access memory as well as thermoelectric materials. The thermal and electrical conductivity of the $Ge_1Sb_4Te_7$ alloy play an important role in both applications. This work aims to determine the thermal conductivity and electrical resistivity of the $Ge_1Sb_4Te_7$ alloy as a function of temperature and to discuss the thermal conduction mechanism. Thermal conductivity and electrical resistivity were measured from room temperature to 778 K using the hot strip method and the four-terminal method, respectively. The thermal conductivity of the $Ge_1Sb_4Te_7$ alloy shows an interesting temperature dependence: it decreases up to about 600 K, and then increases with increasing temperature. The electrical resistivity shows a monotonic increase with increasing temperature. Through a discussion of the thermal conductivity results together with electrical resistivity results, it is proposed that electronic thermal conductivity dominates the thermal conductivity, while the bipolar diffusion contributes to the increase in the thermal conductivity at higher temperatures. The resonance bonding existing in this chalcogenide alloy accounts for the low lattice thermal conductivity.

Key words: $Ge_1Sb_4Te_7$ alloy, thermal conductivity, electrical resistivity, thermal conduction mechanism

INTRODUCTION

$GeTe\text{-}Sb_2Te_3$ pseudo-binary alloys such as $Ge_2Sb_2Te_5$, $Ge_1Sb_2Te_4$, and $Ge_1Sb_4Te_7$ have been widely used for phase-change random access memory (PCRAM) due to their remarkable crystallization kinetics and unique thermophysical properties.[1,2] In PCRAM devices, a precisely controlled amount of heat is provided to fulfill the phase transformation that is the basis of data recording. Fast and localized heating in a minimum area allows lower power consumption and higher scalability of PCRAM applications. In order to carry out the three-dimensional simulation of the time-transient behavior in a PCRAM memory element to obtain the temperature distributions and the heat flow balance, knowledge of the thermal conductivity of $GeTe\text{-}Sb_2Te_3$ pseudo-binary alloys is indispensable.[3]

In addition to the PCRAM applications, $GeTe\text{-}Sb_2Te_3$ pseudo-binary alloys have drawn attention as potential thermoelectric materials. Lead telluride (PbTe)-based materials are considered the leading thermoelectric materials for power generation in the intermediate 600–900-K temperature range.[4–7] The layered intergrowth compounds of the homologous $(PbTe)_m(Bi_2Te_3)_n$ series have been found to have low

(Received May 5, 2016; accepted September 20, 2016; published online October 21, 2016)

thermal conductivity, which is beneficial for thermoelectric applications due to the strong phonon scattering at the interfaces between the layers.[8] However, due to the toxic nature of Pb to the environment, alternative tetradymite-type materials, such as the $(SnTe)_m(Sb_2Te_3)_n$ alloy, have been investigated.[9] GeTe-Sb_2Te_3 pseudo-binary alloys that also feature a layered intergrowth structure have been considered as probable substituents, and have been widely investigated for application in thermoelectric materials.[10–13] The efficiency of a thermoelectric converter is determined by the dimensionless 'thermoelectric figure-of-merit':

$$ZT = \sigma S^2 T/\lambda, \quad (1)$$

where σ, S, and λ are the electrical conductivity, Seebeck coefficient, and thermal conductivity, respectively, and T is the mean operating temperature. The figure of merit is also the ratio of the so-called power factor, σS^2, to the thermal conductivity, λ. It is well known that electronic thermal conductivity is related to electrical conductivity by the Wiedemann–Franz (WF) law.[14]

$$\lambda = L\sigma T, \quad (2)$$

where L is the Lorenz number, which is equal to 2.44×10^{-8} WΩ/K^2 for degenerate and 1.48×10^{-8} WΩ/K^2 for non-degenerate statistics. Hence, to enhance the thermoelectric performance of a certain material, a combination of a high power factor and low lattice thermal conductivity must be obtained. Therefore, clarification of the thermal conduction mechanism of the GeTe-Sb_2Te_3 chalcogenide alloy will be beneficial for tailoring the thermoelectric properties of materials.

There have been some investigations of the thermal conductivity of GeTe-Sb_2Te_3 pseudo-binary alloys; however, most of these studies have focused on the properties of the $Ge_2Sb_2Te_5$ alloy.[15–18] Few data are available for the $Ge_1Sb_4Te_7$ alloy. To our knowledge, only one study has reported on the thermal conductivity of this alloy, which was measured at room temperature using the photoacoustic method.[19] In our previous work, the thermal conductivity of the two binary alloys, Sb_2Te_3[20] and GeTe[21] alloy and the binary Sb-Te alloy system,[22] were investigated. The thermal conductivity of the Sb_2Te_3 alloy shows interesting temperature dependence: it decreases with increasing temperature until about 600 K, and then increases. The Sb-Te binary system shows a similar temperature dependence. However, another binary alloy in the GeTe-Sb_2Te_3 pseudo-binary system, GeTe, shows a different temperature dependence: it decreases monotonously with increasing temperature. The present work is focused on exploring the temperature dependence of the thermal conductivity for the $Ge_1Sb_4Te_7$ alloy.

The difference in electrical resistivity between amorphous and crystalline phases of GeTe-Sb_2Te_3 alloys is the basis of data recording for PCRAM. Electrical resistivity is also an important factor in discussing both the thermal conduction mechanism and the thermoelectric performance. The electrical resistivity of the $Ge_1Sb_4Te_7$ alloy was investigated by Konstantinov et al.[23] However, electrical resistivity is strongly dependent on the composition of the alloy, since exact stoichiometry is difficult to maintain.

Consequently, this work aims to measure the thermal conductivity and electrical resistivity of the $Ge_1Sb_4Te_7$ alloy as a function of temperature. The thermal conduction mechanism will be discussed based on the thermal conductivity and electrical resistivity results.

EXPERIMENTAL

Sample

Cylindrical $Ge_1Sb_4Te_7$ samples were prepared from Sb_2Te_3 (99.9 wt.%) and GeTe (99.9 wt.%) powders. A powder mixture with the desired composition was precisely weighed and melted in quartz crucibles at 1073 K for 4 h in a vacuum. The samples were then cooled at a rate of 50 K/h. The surface of the molten samples was kept below the maximal temperature position of the furnace, so that solidification proceeded from the bottom to the top of the samples, and gas existing in the samples could escape without leaving pores in the samples. The samples for thermal conductivity measurements were cut into two parts along the longitudinal axis. Mechanical polishing was performed using emery papers up to #2000 on the cross sections of samples for thermal conductivity measurements and the surface of samples for electrical resistivity measurements. The crystallographic structures of the $Ge_1Sb_4Te_7$ samples were analyzed by x-ray diffraction (XRD), and the element distributions were analyzed by scanning electron microscopy with an energy-dispersive x-ray spectrometer (SEM–EDS). X-ray fluorescence (XRF) analysis was used to measure the chemical composition of the samples.

Thermal Conductivity Measurements

Thermal conductivity was measured in the radial direction of the samples by the hot strip method,[24–28] which is a type of non-stationary method for thermal conductivity measurement. This method can minimize the radiative losses from the heat source and directly provide thermal conductivity results without using other physical properties, thus reducing errors arising from the measuring and calculation process, especially with high temperatures. A schematic diagram of the hot strip method used is shown in Fig. 1.[21] The setup was described in detail in a previous work.[21] Briefly, a hot strip of Pt-13%Rh (40 mm length, 1 mm width and 100 μm thickness) was sandwiched between two parts of the sample. Two pieces of mica film (20–30 μm thickness) were used for insulation between the hot strip and the sample. The hot strip served as

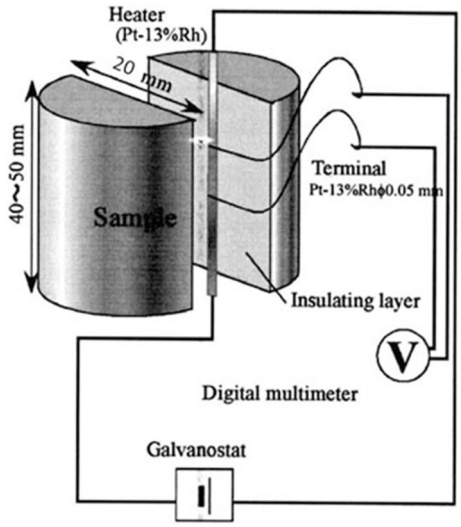

Fig. 1. Schematic diagram of the hot strip method.[21]

both a heating element and a temperature sensor, and the increase in temperature (ΔT) of the hot strip was recorded continuously by two potential leads. On the basis of the solution of a continuous strip source of heat, the thermal conductivity (λ) of the sample was calculated from the equation:

$$\lambda = \frac{Q}{4\pi} \Big/ \frac{d\Delta T}{d \ln t}, \tag{3}$$

where Q is the heat generation rate per unit length of the hot strip and t is time. Thermal conductivity measurements were conducted in an argon atmosphere at temperatures from 298 K to 778 K during both cooling and heating cycles.

Electrical Resistivity Measurements

The four-terminal method was used to measure the electrical resistivity of the $Ge_1Sb_4Te_7$ alloy. Figure 2 shows a schematic of the experimental setup,[21] which was described in detail in a previous work.[21] Briefly, W wires 0.3 mm in diameter were used as the electrodes and were fixed to the sample with alumina cement. The distance between the inner electrodes was about 40 mm, and the distance between the inner and outer electrodes was about 10 mm. The current (I) was supplied between the outer electrodes, and the potential difference (ΔV) was measured between the inner electrodes. The electrical resistance (R) of the sample between the inner electrodes can be derived on the basis of Ohm's law. The electrical resistivity of the sample can be derived using the resistance from the equation:

$$\rho = \frac{R \cdot A}{l} = \frac{\Delta V \cdot A}{I \cdot l}, \tag{4}$$

where A and l represent the cross-sectional area and the distance between the inner electrodes,

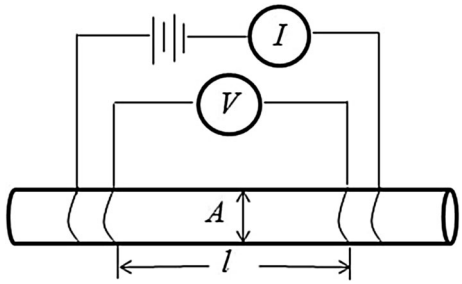

Fig. 2. Conceptual diagram for the four-terminal method.[21]

respectively. Electrical resistivity measurements were conducted in a vacuum atmosphere at temperatures from 298 K to 778 K during both cooling and heating cycles. The supplied electric currents were −0.3 A to +0.3 A.

RESULTS AND DISCUSSION

Comparisons of the XRD and XRF results between the samples of the thermal conductivity and electrical resistivity measurements are shown in Fig. 3 and Table I, respectively. It is clear that the structures checked by XRD and the chemical composition checked by XRF are quite close to each other for these two kinds of samples, which indicates that there is no distinct difference between the samples used for thermal conductivity and electrical resistivity measurements. The $Ge_1Sb_4Te_7$ alloy in the present work is identified from the XRD profiles and the EDS mapping result as a single-phase alloy. The XRD pattern shows diffraction peaks assigned to a rhombohedral structure that is the structure of $Ge_{0.95}Sb_{2.01}Te_4$ alloys. The practical composition is roughly $Ge_{10}Sb_{40}Te_{55}$, but is slightly different from the corresponding nominal composition.

Figure 4a and b shows typical increases in the temperature of the hot strip as a function of the logarithm of time at 298 K and 778 K, respectively. Good linearity can be seen between ΔT and ln$t$ within a reasonable time range, which supports the reliability of the present measurements. ΔT deviates from linearity in the short and long time range. The deviation in the former period is due to the IR drop and the heat capacity of the hot wire, whereas the deviation in the latter period is due to the heat reflection from the sample fixture. The accuracy of the hot strip method has been validated by measuring standard samples, which was published elsewhere.[22] The thermal conductivity of the $Ge_1Sb_4Te_7$ alloy was calculated from Eq. 3, using the slope of the linear portion during the period 0.7–2.0 s, with results of 1.96 $Wm^{-1}\,K^{-1}$ at 298 K and 2.0 $Wm^{-1}\,K^{-1}$ at 778 K.

Figure 5a and b shows typical voltages as a function of current obtained in the measurements for the $Ge_1Sb_4Te_7$ alloy at 298 K and 778 K by the four-terminal method. There is good linearity

between the current and the voltage, which supports the reliability of the present measurements. The electrical resistivity of the $Ge_1Sb_4Te_7$ alloy was calculated using the derived resistance values on the basis of Eq. 4, with results showing electrical resistivity of 1.97×10^{-6} Ωm at 298 K and 8.75×10^{-6} Ωm at 778 K.

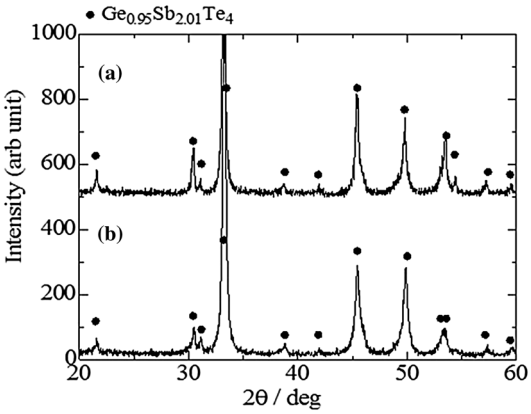

Fig. 3. XRD profile comparison of samples for (a) thermal conductivity and (b) electrical resistivity measurements.

Table I. XRF results comparison of samples for (a) thermal conductivity and (b) electrical resistivity measurements

	mol.% Ge	mol.% Sb	mol.% Te
Nominal	8.33	33.3	58.3
$Ge_1Sb_4Te_7$ (a)	10.07	37.98	51.95
$Ge_1Sb_4Te_7$ (b)	10.06	35.23	54.71

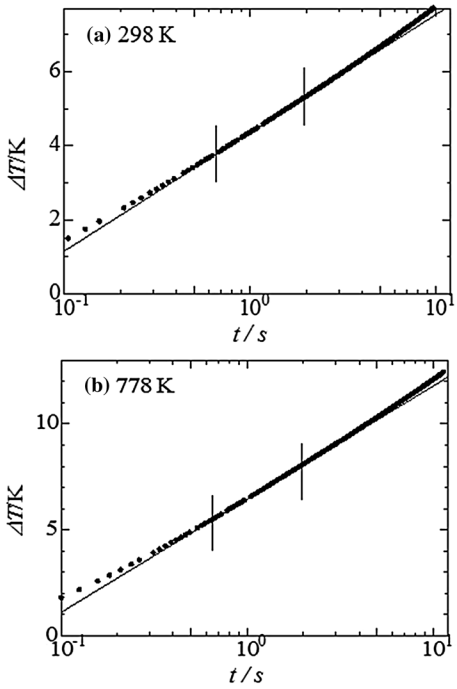

Fig. 4. Rise in temperature of hot strip with time for thermal conductivity measurements of $Ge_1Sb_4Te_7$ at (a) 298 K and (b) 778 K.

Figure 6 shows the temperature dependence of electrical resistivity of the $Ge_1Sb_4Te_7$ alloy, together with the data reported by Konstantinov et al,[23] who studied the electrical resistivity of $Ge_{1-\delta}Sb_{4+\gamma}Te_7$ alloys. The possible range of electrical resistivity for the reported data is given by two lines in Fig. 6. The upper line shows the electrical resistivity data of the $Ge_1Sb_{4.10}Te_7$ alloy, and the lower line shows those of the $Ge_{0.96}Sb_4Te_7$ alloy. The experimental uncertainty of the four-terminal method was determined to be ±3%. Here, one can see that the electrical resistivity of the $Ge_1Sb_4Te_7$ alloy increases with increasing temperature, and is smaller than the lowest limit of the reported data. The difference in the composition of the $Ge_1Sb_4Te_7$ samples used in these two studies is believed to account for the difference in values. The reported data show an anomaly in the range 670–740 K and a sharp decrease at 750 K. The former is due to the phase transitions, and the latter is attributable to the transition to intrinsic conduction mentioned by the authors.[23] Such an anomaly was not found in the present work, which is consistent with the phase diagram for the Sb_2Te_3-GeTe system.[29]

As introduced in Eq. 2, electronic thermal conductivity is related to electrical conductivity by the Wiedemann–Franz (WF) law.[14] Therefore, the electronic component of thermal conductivity can be

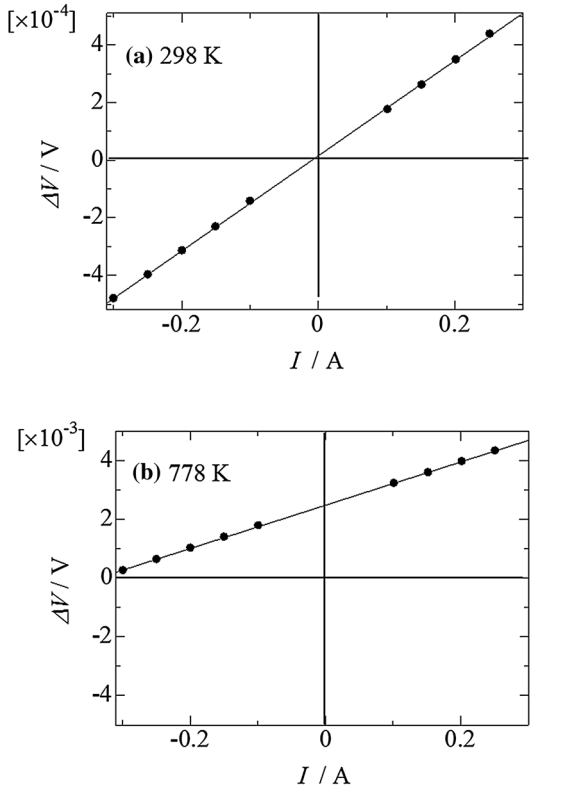

Fig. 5. Typical voltages as a function of current obtained at (a) 298 K and (b) 778 K.

easily obtained using the electrical resistivity results shown in Fig. 6 by Eq. 2. Figure 7 shows the thermal conductivities of the $Ge_1Sb_4Te_7$ alloy measured in this work and the electronic thermal conductivity calculated from the WF law using the Lorenz number 1.48×10^{-8} WΩ/K^2 for non-degenerate semiconductors.[14] The line labeled 'WF law in this work' was calculated using the electrical resistivity results obtained in this work, and that labeled 'WF law by Konstantinov' using the data reported by Konstantinov et al.[23] The experimental uncertainty of the hot strip method was determined to be ±6%. One can see that the thermal conductivity values of the $Ge_1Sb_4Te_7$ alloy have an interesting temperature dependence: they decrease almost linearly with increasing temperature up to approximately 600 K, and then increase. This temperature dependence is similar to that of the Sb_2Te_3 alloy,[20] but different from that of the GeTe alloy.[21] The thermal conductivity values obtained in this work are apparently larger than the highest limit of the 'WF law by Konstantinov', but close to the line 'WF law in this work'. At near room temperature, the thermal conductivity values are smaller than those of 'WF law in this work', which seems impossible, since the lattice thermal conductivity must exist except the electronic thermal conductivity. Practice has shown that the use of the theoretical value of the Lorentz number is not suitable for the calculation of all alloys, since its absolute value changes depending upon the type of material and the temperature. Although the electronic component of the thermal conductivity could not be precisely distinguished, we are still able to deduce that the electronic thermal conductivity dominates the thermal conduction at close to room temperature, and the lattice component can be neglected. The appreciable electronic contribution of the $Ge_1Sb_4Te_7$ alloy may be explained by the considerable number of Ge/Sb vacancies—for example, 20% for the $Ge_2Sb_2Te_5$ alloy.[1] The low lattice thermal conductivity is attributable to the existence of resonance bonding and lattice distortions in the $Ge_1Sb_4Te_7$ alloy. Lee et al.[30] revealed that resonance bonding exhibited long-range interactions in a rock-salt structure using first-principles calculations. This long-range interaction results in optical phonon softening,[31] strong anharmonic scattering, and large phase space for three-phonon scattering processes, which accounts for the low lattice thermal conductivity.

Above room temperature, electronic thermal conductivity decreases monotonically with increasing temperature, whereas the total thermal conductivity begins to increase above about 600 K. In solids, heat is usually transported by electrical carriers and phonons. The lattice thermal conductivity is proportional to the reciprocal of T ($T \gg \Theta_D$, Θ_D is Debye temperature)[14] and also decreases with increasing temperature. Therefore, bipolar diffusion should be considered to explain the increase in thermal conductivity at a higher temperature. During the measurement of thermal conductivity using the hot strip method, a temperature gradient is applied to the sample. The temperature gradient causes the number gradient of electrons and holes to move in a radial direction of the sample, and the electron–hole pairs are transported along the temperature gradient and recombine at the cold end, i.e., sample surface. The energy is transported by heat absorption for ionization at the hot end and heat generation for the recombination of electrons and holes at the cold end.[14] Therefore, bipolar diffusion will contribute an additional electronic part to the total thermal conductivity which rises from the Peltier heat flows, even when the total electric current is zero. The bipolar diffusion is more effective at a higher temperature and contributes to the increased thermal conductivity.

Based on the discussion above, the $Ge_1Sb_4Te_7$ alloy has very low lattice thermal conductivity, which is a key factor in obtaining a high thermoelectric figure of merit. However, the high cation vacancy concentration and bipolar diffusion

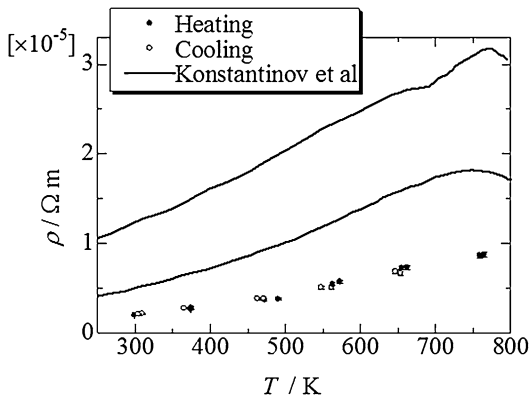

Fig. 6. Electrical resistivity values of the $Ge_1Sb_4Te_7$ alloy as a function of temperature, together with reported data.[23]

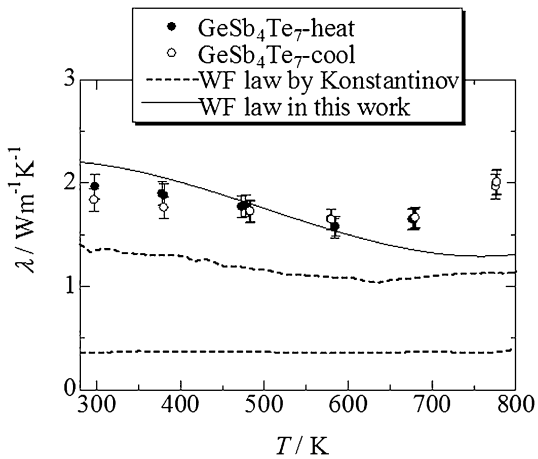

Fig. 7. Thermal conductivity values of the $Ge_1Sb_4Te_7$ alloy, together with values calculated from WF law using electrical resistivity measurements obtained in this work and by Konstantinov et al.[23]

severely impede the enhancement of thermoelectric performance as well as PCRAM applications. A designed doping of donor elements will effectively compensate for the cation vacancy and adjust the charge carrier to the single type. Further investigations of this aspect are suggested.

CONCLUSIONS

In conclusion, the thermal conductivity and electrical resistivity of the $Ge_1Sb_4Te_7$ alloy were measured as a function of temperature, and the thermal conduction mechanism was discussed based on thermal conductivity and electrical resistivity data. From this study, it is proposed that electrical carriers dominate the heat transport due to the high cation vacancy density. Bipolar diffusion plays a role and contributes to the increased thermal conductivity at higher temperatures. Resonance bonding existing in this chalcogenide exhibits a long-range atomic interaction and results in very low lattice thermal conductivity. Further study regarding donor element doping is proposed to improve PCRAM applications and thermoelectric performance.

ACKNOWLEDGEMENT

A portion of the present work was financially supported by the Natural Science Foundation of China (no. 51401090) and the Natural Science Foundation of Jiangsu Province (grant no. BK20140515).

REFERENCES

1. M. Wuttig and N. Yamada, *Nat. Mater.* 6, 824 (2007).
2. N. Yamada, E. Ohno, K. Nishiuchi, and N. Akahira, *J. Appl. Phys.* 69, 2849 (1991).
3. R. Lan, Thermal conductivities and conduction mechanisms of Sb-Te binary and Sb_2Te_3-GeTe pseudobinary chalcogenide alloys. Ph.D. Dissertation, Tokyo Institute of Technology (2012).
4. J. Sootsman, D.Y. Chung, and M.G. Kanatzidis, *Angew. Chem. Int. Ed.* 48, 8616 (2009).
5. G.J. Snyder and E.S. Toberer, *Nat. Mater.* 7, 105 (2008).
6. Y. Pei, X. Shi, A. LaLonde, H. Wang, L. Chen, and G.J. Snyder, *Nature* 473, 66 (2011).
7. K. Biswas, J. He, Q. Zhang, G. Wang, C. Uher, V.P. Dravid, and M.G. Kanatzidis, *Nat. Chem.* 3, 160 (2011).
8. A. Chatterjee and K. Biswas, *Angew. Chem. Int. Ed.* 54, 5623 (2015).
9. A. Banik, B. Vishal, S. Perumal, R. Datta, and K. Biswas, *Energy Environ. Sci.* 9, 2011 (2016).
10. S. Perumal, S. Roychowdhury, D.S. Negi, R. Datta, and K. Biswas, *Chem. Mater.* 27, 7171 (2015).
11. D. Lencer, M. Salinga, B. Grabowski, T. Hickel, J. Neugebauer, and M. Wuttig, *Nat. Mater.* 7, 972 (2008).
12. T. Siegrist, P. Jost, H. Volker, M. Woda, P. Merkelbach, C. Schlockermann, and M. Wuttig, *Nat. Mater.* 10, 202 (2011).
13. E.R. Sittner, K.S. Siegert, P. Jost, C. Schlockermann, F.R.L. Lange, and M. Wuttig, *Phys. Status Solidi Appl. Mater. Sci.* 210, 147 (2013).
14. T.M. Tritt, *Thermal Conductivity: Theory, Properties, and Applications* (New York: Kluwer Academic/Plenum Publishers, 2004), p. 105.
15. V. Giraud, J. Cluzel, V. Sousa, A. Jacquot, A. Dauscher, B. Lenoir, H. Scherrer, and S. Romer, *J. Appl. Phys.* 98, 013520 (2005).
16. H.-K. Lyeo, D.G. Cahill, B.-S. Lee, J.R. Abelson, M.-H. Kwon, K.-B. Kim, S.G. Bishop, and B.-K. Cheong, *Appl. Phys. Lett.* 89, 151904 (2006).
17. J.P. Reifenberg, M.A. Panzer, S.-B. Kim, A.M. Gibby, Y. Zhang, S. Wong, H.-S. Philip Wong, E. Pop, and K.E. Goodson, *Appl. Phys. Lett.* 91, 111904 (2007).
18. W.P. Risk, C.T. Rettner, and S. Raoux, *Appl. Phys. Lett.* 94, 101906 (2009).
19. J.M. Yanez-Limon, J. G-Hernandez, J.J. A-Gil, I. Delgadillo, and H. Vargas, *Phys. Rev. B*, 52, 16321 (1995).
20. R. Lan, R. Endo, M. Kuwahara, Y. Kobayashi, and M. Susa, *Jpn. J. Appl. Phys.* 49, 078003 (2010).
21. R. Lan, R. Endo, M. Kuwahara, Y. Kobayashi, and M. Susa, *J. Appl. Phys.* 112, 053712 (2012).
22. R. Lan, R. Endo, M. Kuwahara, Y. Kobayashi, and M. Susa, *J. Appl. Phys.* 110, 023701 (2011).
23. P.P. Konstantinov, L.E. Shelimova, E.S. Avilov, M.A. Kretova, and V.S. Zemskov, *Inorg. Mater.* 37, 662 (2001).
24. S.E. Gustafsson, E. Karawacki, and M.N. Khan, *J. Phys. D* 12, 1411 (1979).
25. S.E. Gustafsson, E. Karawacki, and M.N. Khan, *J. Appl. Phys.* 52, 2596 (1981).
26. S.E. Gustafsson, *J. Appl. Phys.* 53, 6064 (1982).
27. S.E. Gustafsson, E. Karawacki, and M.A. Chohan, *J. Phys. D* 19, 727 (1986).
28. M. Susa, K. Nagata, and K.S. Goto, *Trans. Jpn. Inst. Met.* 29, 133 (1988).
29. L.E. Shelimova, O.G. Karpinskii, V.S. Zemskov, and P.P. Konstantinov, *Inorg. Mater.* 36, 235 (2000).
30. S. Lee, K. Esfarjani, T. Luo, J. Zhou, Z. Tian, and G. Chen, *Nat. Commun.* 5, 3525 (2014).
31. T. Matsunaga, N. Yamada, R. Kojima, S. Shamoto, M. Sato, H. Tanida, T. Uruga, S. Kohara, M. Takata, P. Zalden, G. Bruns, I. Sergueev, H.C. Wille, R.P. Hermann, and M. Wuttig, *Adv. Funct. Mater.* 21, 2232 (2011).